Hindawi
Geofluids
Volume 2023, Article ID 5093331, 11 pages
https://doi.org/10.1155/2023/5093331

Research Article

The Anisotropy Permeability Evolution and Deformation Behavior of Raw Coal under Cyclic Loading Conditions

Hanhua Xu [1,2]

[1]*Kunming Prospecting Design Institute Of China Nonferrous Metals Industry Co., Ltd, Kunming, China 650051*
[2]*Yunnan Key Laboratory of Geotechnical Engineering and Geohazards, Kunming, China 650051*

Correspondence should be addressed to Hanhua Xu; xuhanhua@cug.edu.cn

Received 30 August 2022; Revised 12 October 2022; Accepted 24 November 2022; Published 20 January 2023

Academic Editor: Peng Tan

As an anisotropic porous media, coal's intrinsic permeability is sensitive to stress variably in different directions. Likewise, the degree of damage sustained by the internal solid skeletal structure under external stresses is anisotropic. Four parameters are introduced: permeability stress-based loss rate (*PEL*) and permeability strain-based loss rate (*PSL*) highlight the stress sensitivity of the intrinsic permeability and deformation characteristics of coal's internal structure during the loading process; stress-based irrecoverable permeability coefficient (*EIP*) and strain-based irrecoverable permeability coefficient (*SIP*) describe the loss of intrinsic permeability and irreversible deformation features in the whole load cycle. Stress sensitivity of the vertical intrinsic permeability is greater than that of the horizontal, and the ability of the vertical internal structure to resist deformation induced by an external load is weaker. During the cyclic loading process for the same coal sample, the stress sensitivity of the latter loading cycle is significantly less than the former.

1. Introduction

During the CBM extraction process, as methane is desorbed, the gas pressure in a coal seam gradually decreases, and the in situ stress changes. The deformation of coal's internal structure changes the reservoir's permeability, which in turn affects the further extraction of CBM. In situ stress and pore pressure play significant roles in the processes of adsorption, desorption, diffusion, and percolation of CBM. Unlike other porous media, coal contains significant numbers of cleats or fractures. It has obvious anisotropic characteristics because of the differences between the face and butt cleat and bedding plane properties and in situ anisotropic stress conditions [1–3]. The difference between the vertical and horizontal permeability is enormous [4–7]. Koenig and Stubbs have reported a differential permeability ratio of 17 : 1 [8]. Wold and Jeffrey [9] conducted a four-well injection interference test to measure the overall seam permeability anisotropy and found that different seams, and even different regions within a composite seam, can have significantly different permeability anisotropy characteristics. Permeability anisotropy plays an important role in the CBM production rate [9, 10] and hydraulic fracture propagation. Many other studies on coal's permeability anisotropy with respect to different stresses can be found in the review published by Pan and Connell [11]. However, a systematic study on the evolution of coal's intrinsic permeability anisotropy under cyclic loading conditions is still lacking, which is of great significance.

Many scholars have researched the deformations of coal's internal structure and the dynamic evolution of permeability during CBM production. Pan et al. [7] studied the permeability of an Australian coal from the Sydney Basin using three different gases—*He*, CH_4, and CO_2—and coal's corresponding deformation characteristics. Coal permeability is sensitive to stress, and cleat compressibility is often used to describe the sensitivity of permeability to stress for coal reservoirs [12, 13]. Cleat compressibility is a measure of the cleat volume change ratio with respect to pore pressure change, which is defined in the following:

$$C_f = \frac{1}{\varphi}\frac{\partial \varphi}{\partial P}, \tag{1}$$

where C_f is the cleat compressibility, φ is the porosity, and P is the pore pressure.Cleat compressibility is often obtained by fitting experimental data using exciting permeability models [14]. However, cleat compressibility is not constant with respect to pore pressure and effective stress [13, 15]. Dynamic cleat compressibility is not easy to obtain during the penetration process when external stress changes. Experimental studies are still lacking on the stress sensitivity of intrinsic permeability combined with strain characteristics. In addition, the stress sensitivity of coal's intrinsic permeability in different directions with respect to cyclic stresses is not yet well studied.

Gas migration in coal is a combined process in which gas flow and the internal solid structure interact with each other. This process becomes more complex due to the gas slippage effect [16]. It was first proposed by Klinkenberg in 1941, which means when gas is penetrating in channels of porous media, the gas molecules close to cell walls show no zero flow rate [17]. It reflects the effect of gas pressure on gas permeability. The mathematical expression can be found in the following:

$$K_g = K\left(1 + \frac{b}{p}\right), b = \frac{4c}{\gamma}\lambda p, \tag{2}$$

where P is the average pore pressure; K_g is the gas permeability; K is the Klinkenberg or intrinsic permeability; b is the Klinkenberg factor, depending on the mean free path of the gas molecules, which, in turn, depends on the pressure, temperature, and molecular weight of the gas [17, 18]; c is a scale factor; λ is the mean free path of the gas molecules, and γ is the average pore radius. When $b = 0$, gas slippage has no effect on permeability, and the penetration follows Darcy's law. The gas slippage effect has a large impact on penetration, especially in low permeability reservoirs. The existence of slippage is good for raising reservoir permeability, which makes possible the exploitation of large-scale low permeability coalbed methane reservoirs. However, the slippage effect also has its limitations. It has been observed that the gas slippage effect diminishes as gas pressure increases because at high pressures (e.g., >2 MPa), the mean free path of the gas molecules (diameter approximately 0.98 Å) is far less than the aperture of the coal cleats (3–40 um) [19].

In this paper, the contributions are mainly reflected in following three aspects. (1) The permeability anisotropy behaviors for low-rank coal samples (long-flame coal), namely, parallel and perpendicular to coal bedding, were studied by N_2 under cyclic loading conditions. Intrinsic permeability under different triaxial stresses was obtained by calculating and removing the impact of the gas slippage effect. (2) Four parameters are introduced in this work: permeability stress-based loss rate (*PEL*), stress-based irrecoverable permeability coefficient (*EIP*), permeability strain-based loss rate (*PSL*), and strain-based irrecoverable permeability coefficient (*SIP*). *PEL* and *PSL* feature the stress sensitivity of intrinsic permeability and deformation characteristics of coal's internal structure during the loading process, while *EIP* and *SIP* describe the loss of intrinsic permeability and plastic or irreversible deformation features of the whole load cycle. (3) By analyzing the evolutionary law of coal permeability anisotropy with respect to cyclic stresses, combined with the *PEL*, *EIP*, *PSL*, and *SIP* results, the mechanical characteristics of coal's internal structure were investigated.

2. Experimental Methods

2.1. Sample Preparation and Test Apparatus. Long-flame coal was chosen as our experimental object, among developed multiminable coal seams. The average bulk density is 1340 kg/m^3. The majority of macerals are vitrinite (78.59%). Coal permeability anisotropy was studied with two types of coal samples: sample C3 was parallel to the bedding, while samples C1 and C2 were perpendicular to the bedding. All samples were trimmed to a dimension of Φ50 $\times$ 100 mm.

The steady-state method was used to measure the permeability of coal along with the low-permeability rock permeability test system. The average pore pressure is approximately the average of inlet and outlet gas pressures.

2.2. Experimental Procedure. The permeability of coal samples was tested by N_2 under different gas pressures and cyclic external loading conditions. The cyclic loading process can be divided into two sections: cyclic hydrostatic stresses and cyclic deviatoric stresses, during which confined stresses of 8 MPa and 14 MPa, respectively, are maintained.

3. Experimental Results

Generally, horizontal permeability is greater than vertical. Figure 1 shows the coal samples' permeability test results under different hydrostatic stresses. The magnitude of horizontal permeability tested in samples C1 and C2 is 1 ~ 2 orders larger than the vertical permeability tested in C3. This shows that apparent permeability decreases exponentially as pore pressure increases, which has been confirmed by many other studies [20] and is partly caused by the slippage effect.

Figure 2 depicts the apparent permeability evolution of sample C1 under cyclic axial stresses while maintaining a confined pressure of 8 MPa and 14 MPa. Apparent permeability decreases when hydrostatic stress or axial stress increases and increases during unloading. The slope of the loading curve is significantly larger than that of unloading, and plastic deformation is generated at each stress cycle. Details of the test results can be found in our previous study [21].

The Klinkenberg effect is an important phenomenon for gas flow in low permeability reservoirs, and its influence increases as gas pressure is reduced. Intrinsic permeability under different stresses was obtained by calculating and removing the impact of the gas slippage effect. As opposed to apparent permeability, intrinsic permeability remains constant if no variation occurs to coal's internal pore structure. In other words, intrinsic permeability only relates to structural properties (the average particle size, porosity, etc.) of the porous medium itself and has no connection to

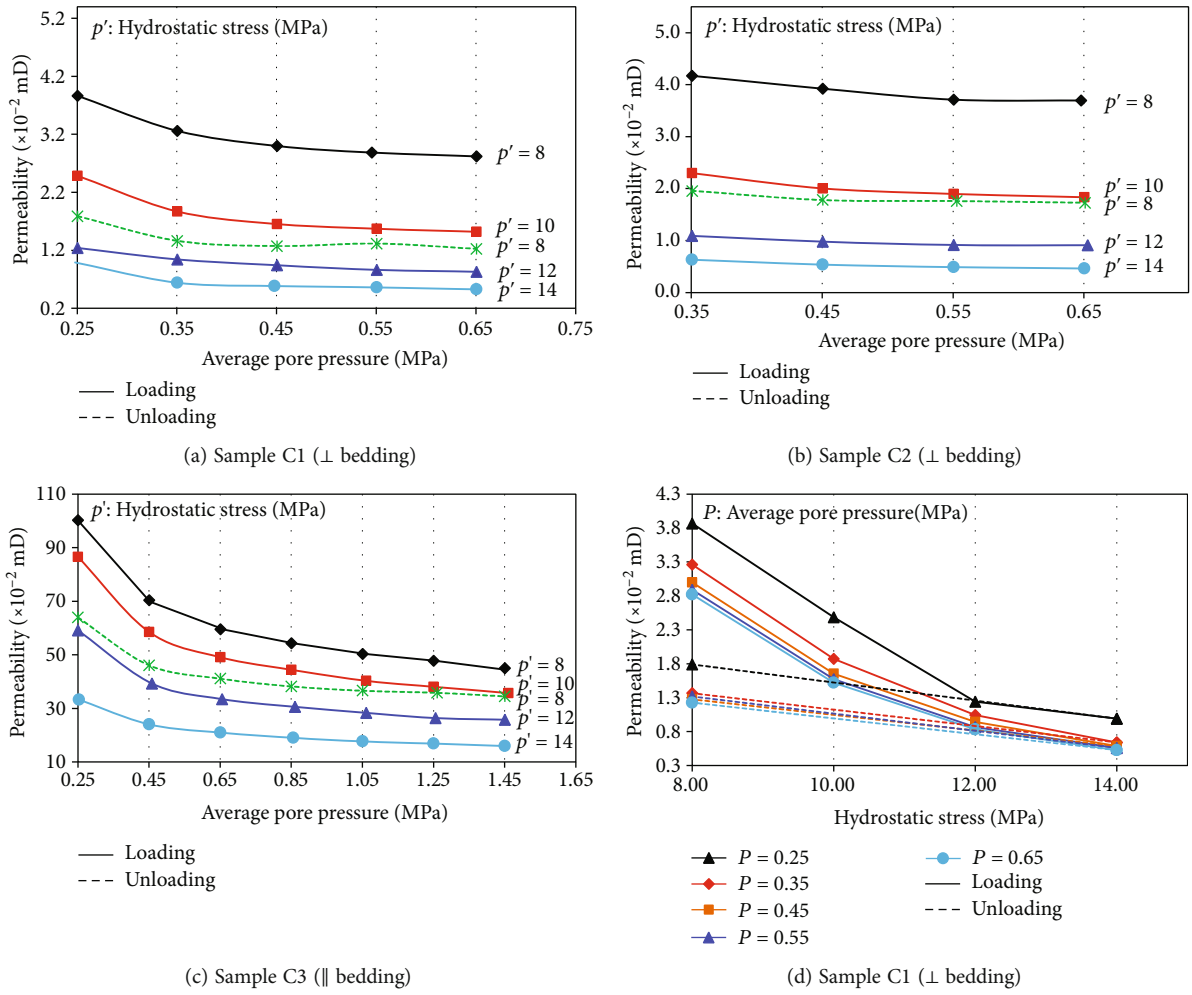

Figure 1: The permeability test results of coal samples under hydrostatic stresses.

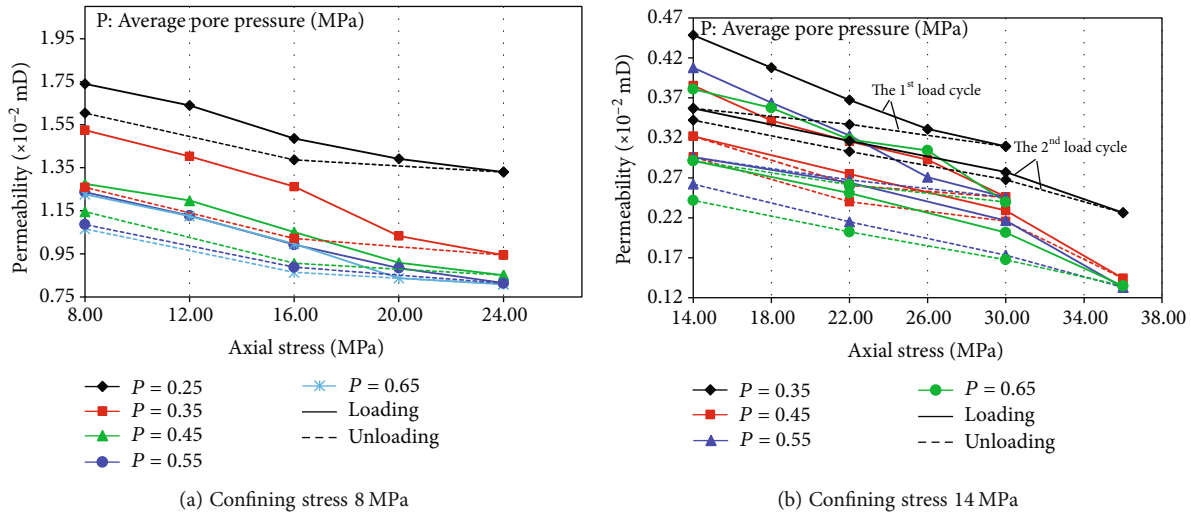

Figure 2: The permeability test results of coal sample C1 under hydrostatic stresses.

the characteristics of single-phase Newtonian's fluids. Intrinsic permeability is constant when tested by different single-phase Newtonian's fluids [22]. Intrinsic permeability is obtained by fitting the slippage effect expression Equation (2) with the experimental results of apparent permeability. The slippage fitting process of sample C1 under hydrostatic

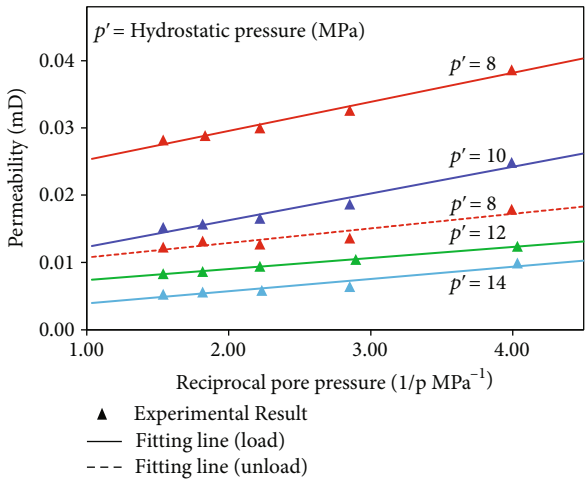

Figure 3: The slippage effect fitting process of sample C1 under hydrostatic stress.

Table 1: Coal intrinsic permeability under different hydrostatic stresses ($\times 10^{-2}$ mD).

Samples	Hydrostatic stress loading condition				Unloading condition
	8 MPa	10 MPa	12 MPa	14 MPa	8 MPa
C1	2.09	0.84	0.57	0.21	0.87
C2	3.06	1.26	0.67	0.26	1.44
C3	34.34	25.73	18.72	12.67	28.03

stresses is shown in Figure 3 and is similar to deviatoric stress conditions and other samples. Apparent permeability increases linearly with reciprocal pore pressure. The final intrinsic permeability results are listed in Tables 1–3.

4. Evolution of Intrinsic Permeability and Deformation Behavior

During CBM extraction or coal and methane common mining, complicated changes occur in the mining stress field, and then porosity changes, eventually leading to a dynamic evolution of coal seam permeability. Compressed deformation caused by in situ stress changes may lead to permanent damage in coal's internal skeletal structure and its intrinsic permeability. Coal permeability is typically anisotropic because of differences between the face and butt cleat and bedding plane properties and in situ anisotropic stress conditions [1, 11]. The loss of intrinsic permeability in different directions and the corresponding damage deformation during cyclic loading conditions are significantly different. By studying coal's intrinsic permeability and strain evolution during the cyclic loading process, this study provides a better understanding of the stress sensitivity of intrinsic permeability in different directions and deformation characteristics of coal.

4.1. Introduction of Evaluated Parameters. To study the stress sensitivity of intrinsic permeability and deformation characteristics during the loading process, the terms permeability stress-based loss rate (*PEL*) and permeability strain-based loss rate (*PSL*) are introduced. Additionally, the terms stress-based irrecoverable permeability coefficient (*EIP*) and strain-based irrecoverable permeability coefficient (*SIP*) are introduced to describe the loss in intrinsic permeability and plastic or irreversible deformation features of the whole loading cycle. This study uses these four parameters to describe quantitatively and interpret the changes in coal's internal structure.

4.1.1. Permeability Stress-Based Loss Rate (PEL). PEL is used to define the dynamic loss rate of intrinsic permeability when unit stress increases during the loading process, which is expressed as

$$\mathrm{PEL} = \frac{K_i - K_{i+1}}{K_0(P_{i+1} - P_i)}, \tag{3}$$

where K_i and K_{i+1} represent intrinsic permeability in the i_{th} and $i + 1_{\mathrm{th}}$ load, respectively; K_0 is the initial intrinsic permeability; and P_i and P_{i+1} are the i_{th} and $i + 1_{\mathrm{th}}$ external stresses. The larger the PEL, the more sensitive intrinsic permeability is to applied stress.

4.1.2. Stress-Based Irrecoverable Permeability Coefficient (EIP). EIP is defined to describe the irreversible damage to the intrinsic permeability of the whole load cycle, which is expressed as

$$\mathrm{EIP} = \frac{K_0 - K_0{}'}{K_0\sigma_{\max}}, \tag{4}$$

where K_0 is the initial intrinsic permeability, $K_0{}'$ is the intrinsic permeability when the whole load cycle is finished and then returned to its initial stress state, and $\sigma_{\max}$ is the difference between the maximum stress during the loading process and the initial stress.

The larger the EIP, the greater is the irreversible loss in intrinsic permeability under the maximum differential stress $\sigma_{\max}$.

4.1.3. Permeability Strain-Based Loss Rate (PSL). *PSL* is used to define the dynamic loss rate of intrinsic permeability when unit strain increases during the loading process. The connection between coal's macroscopic deformation and the variation in intrinsic permeability is established by *PSL*. It is beneficial for studying the mechanical deformation features of coal's internal structure. PSL is expressed as

$$\mathrm{PSL} = \frac{K_i - K_{i+1}}{K_0(\varepsilon_{i+1} - \varepsilon_i)}, \tag{5}$$

where ε_i and ε_{i+1} represent intrinsic permeability in the i_{th} and $i + 1_{\mathrm{th}}$ load, respectively. The unit is %.

4.1.4. Strain-Based Irrecoverable Permeability Coefficient (SIP). *SIP* is defined as the irreversible loss rate of coal's intrinsic permeability when the unit irreversible strain increases for the whole loading cycle. It is a measure of the

Table 2: Coal intrinsic permeability under different deviatoric stresses when confining stress 8 MPa ($\times 10^{-2}$ mD).

Samples	Axial stress loading condition					Unloading condition	
	8 MPa	12 MPa	16 MPa	20 MPa	24 MPa	16 MPa	8 MPa
C1	0.97	0.74	0.54	0.35	0.22	0.33	0.53
C2	1.54	1.14	0.78	0.47	0.25	0.54	0.85
C3	28.63	24.92	21.68	19.08	16.66	17.34	21.59

Table 3: Coal intrinsic permeability under different deviatoric stresses when confining stress 14 MPa ($\times 10^{-2}$ mD).

Samples	The 1st loading					The 1st unloading		The 2nd loading					The 2nd unloading			
	Axial stress (MPa)					Axial stress		Axial stress (MPa)					Axial stress (MPa)			
	14	18	22	26	30	22	14	22	30	34	36	41	36	30	22	14
C1	0.32	0.27	0.24	0.21	0.14	0.16	0.21	0.17	0.11	—	0.01	—	0.01	0.04	0.07	0.10
C2	0.27	0.17	0.11	0.08	0.02	0.07	0.13	0.07	0.01	—	—	—	—	0.01	0.05	0.10
C3	8.11	7.25	6.46	5.73	5.20	5.38	6.56	5.55	4.93	4.51	—	3.42	3.43	3.69	4.01	4.53

permanent damage or the irreversible intrinsic permeability during the cyclic loading process. It is expressed as

$$\mathrm{SIP} = \frac{\left(K_0 - K_0{}'\right)}{K_0\left(\varepsilon_0{}' - \varepsilon_0\right)}, \tag{6}$$

where ε_0 is the initial strain (the unit is %), and $\varepsilon_0{}'$ is the strain after the whole load cycle is finished and returned to its initial stress state.

4.2. Evolution of Intrinsic Permeability and Deformation Behavior under Hydrostatic Stresses. Figure 4 shows the evolution of intrinsic permeability and the axial strain of coal samples under cyclic hydrostatic stresses. Apparently, intrinsic permeability decreases significantly when hydrostatic stress increases from 8 MPa to 14 MPa and then increases when the hydrostatic stress decreases.

Figure 5 shows intrinsic permeability decreasing exponentially when the strain increases. When the strain recovers, intrinsic permeability is lower than it was during the loading process. Plastic deformation and permanent damage happen to coal's internal pore structure or solid skeleton.

The *PEL* and *PSL* of coal in different directions under cyclic hydrostatic stresses are calculated and shown in Figure 6. From Figure 6(a), it can be observed that *PEL* decreases sharply in the early stage of loading and then levels off after 12 MPa. *PEL* results indicate that as hydrostatic stress increases, intrinsic permeability becomes more insensitive to stress. When an external load is applied, coal and other rock will be compacted and deformed first; the original pores and fractures are partially closed under stress [23–26]. During this process, the ability of coal's internal skeletal structure to resist deformation is so weak that its intrinsic permeability decreases rapidly. At the later stage, the compressive deformation rate of coal's internal structure becomes relatively stable. The reduction in porosity and permeability decreases at the same stress increment. Vertical *PEL* is obviously larger than horizontal *PEL* when hydrostatic stress is 10 MPa. Under relatively higher stresses (12 or 14 MPa), the *PEL* is very close in both directions. In the early stages of loading, the stress sensitivity of the vertical intrinsic permeability is greater than that of the horizontal.

PSL curves have similar trends as *PEL*, as shown in Figure 6(b). *PSL* analyzes the deformation of the internal structure and the evolution of intrinsic permeability from the strain perspective. It shows the dynamic loss rate of intrinsic permeability when the unit strain increases during the loading process. As coal is compacted and deformed, the compression of its internal pore structure contributes greatly to the overall strain, resulting in a significant loss of porosity and intrinsic permeability. When hydrostatic stress increases, the compressive deformation rate of coal's internal structure slows, such that intrinsic permeability eventually loses stability.

Coal's internal structure would be damaged under cyclic loading conditions, and irreversible deformation would take place. The loss of intrinsic permeability and the plastic deformation features of the whole load cycle can be described by *EIP* and *SIP*. Based on Equation (4), the *EIP* of sample C1 is 0.098, that of C2 is 0.088, while that of C3 is only 0.031. The irreversible intrinsic permeability loss rate of coal in the vertical direction is significantly greater than that in a parallel direction under cyclic hydrostatic stress 8 $\longrightarrow$ 14 $\longrightarrow$ 8 MPa. The strain-based irrecoverable permeability coefficient (*SIP*) of sample C1 is 77.35, that of C2 is 63.58, and that of C3 is 26.63. Due to the damage sustained by the coal's internal structure, it cannot recover from part of the strain at the end of cyclic loading. The *SIP* of coal in the vertical direction is significantly higher than the horizontal. So, given the same plastic deformation, the loss of intrinsic permeability in different directions is different. This is attributed to the anisotropic mechanical characteristics of coal. The results of *EIP* and *SIP* indicate that the ability of

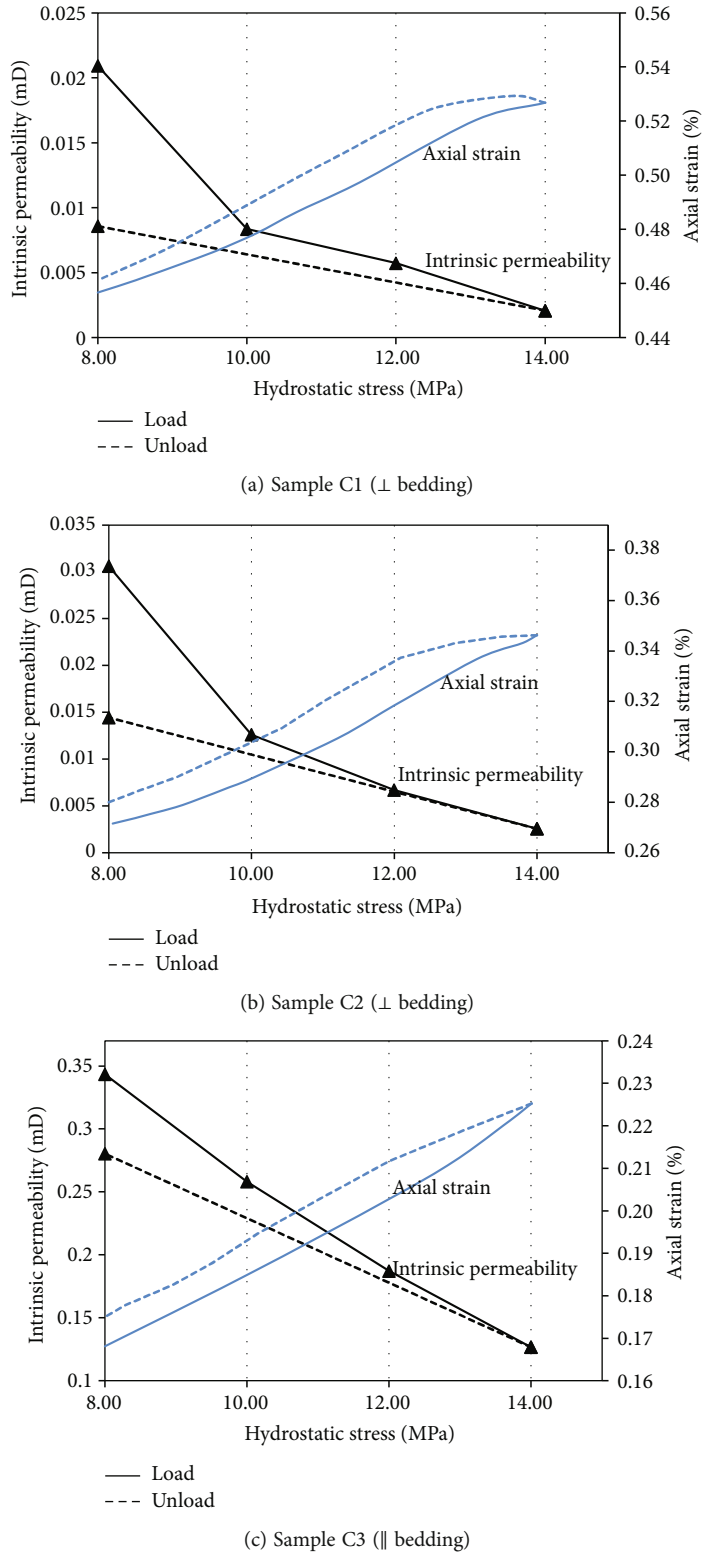

Figure 4: The evolution of intrinsic permeability and axial strain under cyclic hydrostatic stresses.

coal's internal structure to resist deformation induced by hydrostatic stress vertically is weaker than it is horizontally.

4.3. Evolution of Intrinsic Permeability and Deformation Behavior under Deviatoric Stresses. To study the sensitivity of coal's intrinsic permeability to deviatoric stress, permeability under cyclic axial stresses was tested by maintaining confining stress at 8 MPa and 14 MPa. To study the impact of peak stress during the cyclic loading process on the intrinsic permeability and deformation characteristics, the stress

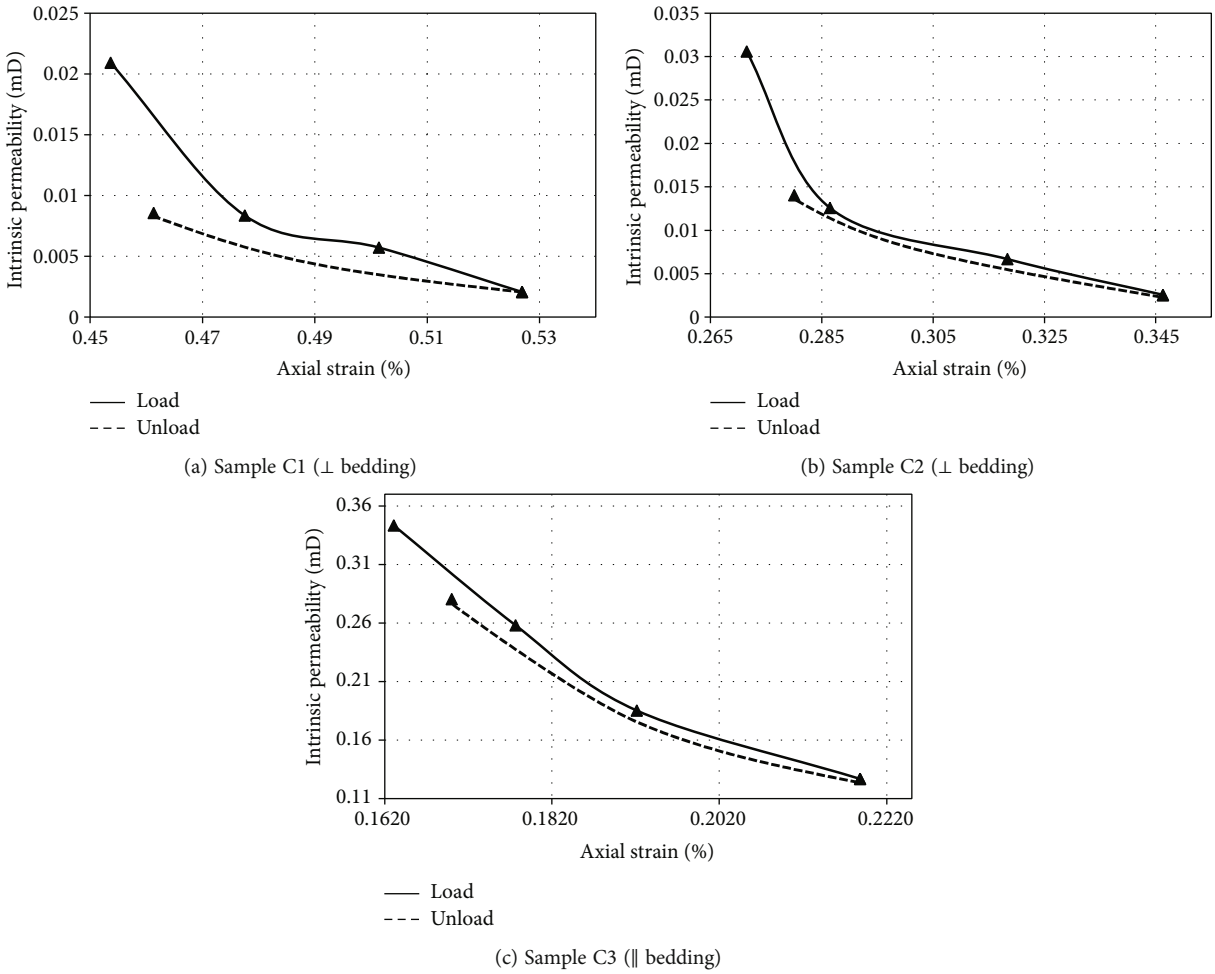

Figure 5: Intrinsic permeability changes with strain during cyclic loading.

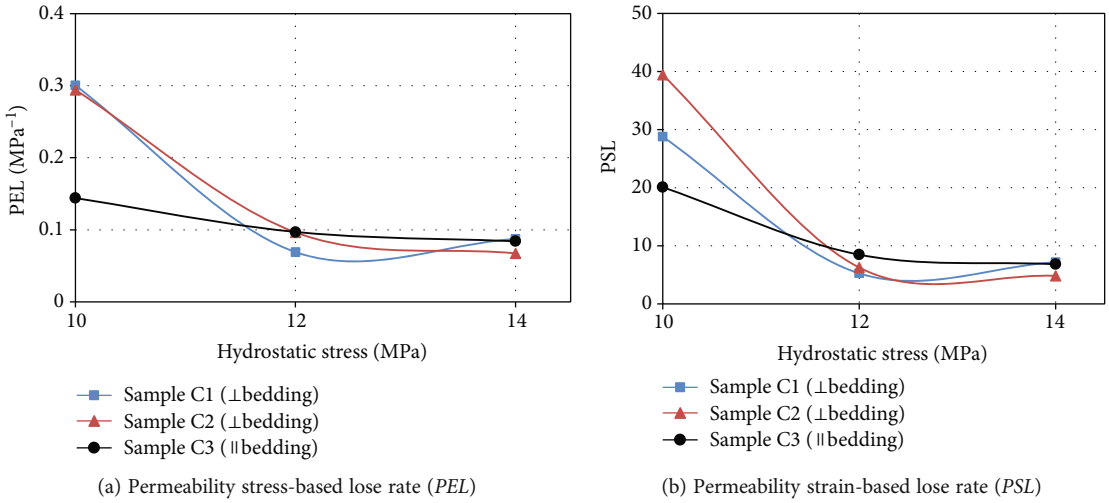

Figure 6: *PEL* and *PSL* of coal samples in different directions under cyclic hydrostatic stresses.

paths of the 2nd load cycle were varied when confining pressure is at 14 MPa.

Intrinsic permeability evolution of sample C1 under different deviatoric stresses is shown in Figure 7. Subsets, (a)-(c) maintain confining stress at 8 MPa, while subsets (d)-(f) maintain confining stress at 14 MPa. It can be observed from the figure that intrinsic permeability could not completely recover after cyclic axial stress.

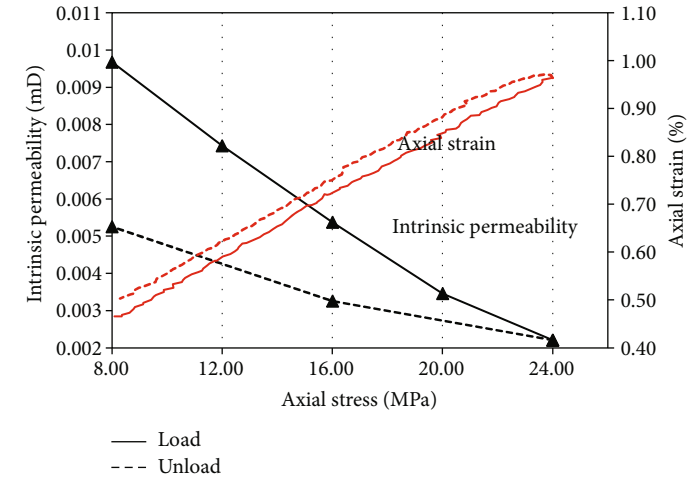

(a) Sample C1 under confining stress 8 MPa (⊥ bedding)

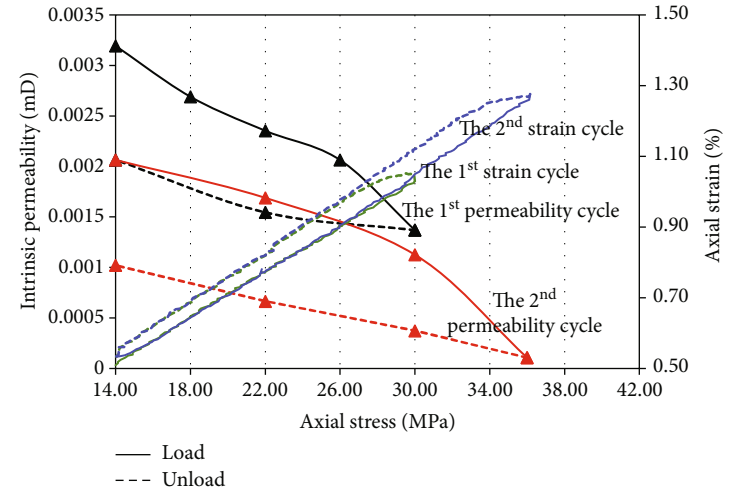

(b) Sample C1 under confining stress 14 MPa (⊥ bedding)

Figure 7: Coal intrinsic permeability evolution under deviatoric stresses.

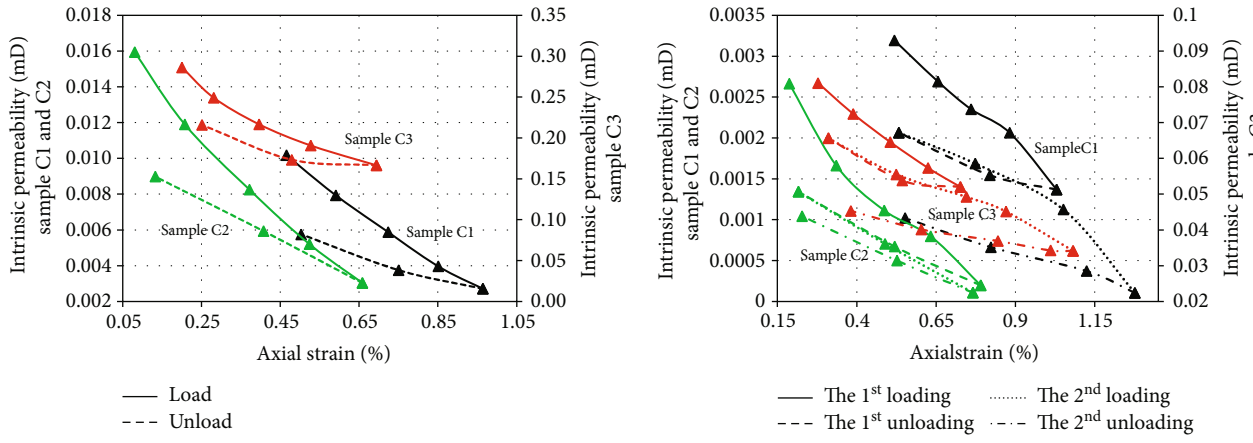

(a) Confining stress 8 MPa

(b) Confining stress 14 MPa

Figure 8: Coal intrinsic permeability changes with strain during cyclic axial stresses.

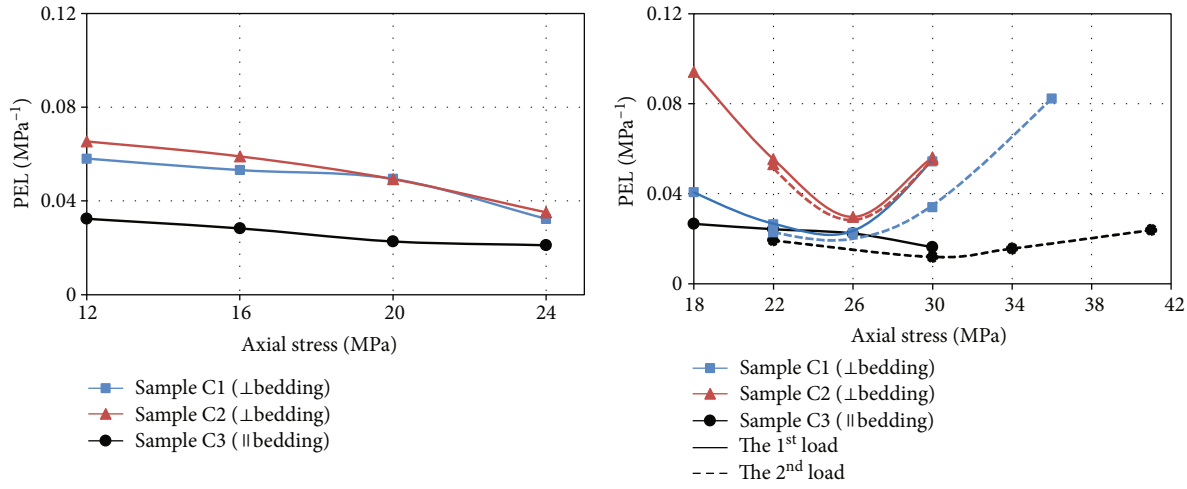

(a) Confining stress 8 MPa (b) Confining stress 14 MPa

Figure 9: The *PEL* calculating results under cyclic deviatoric stresses.

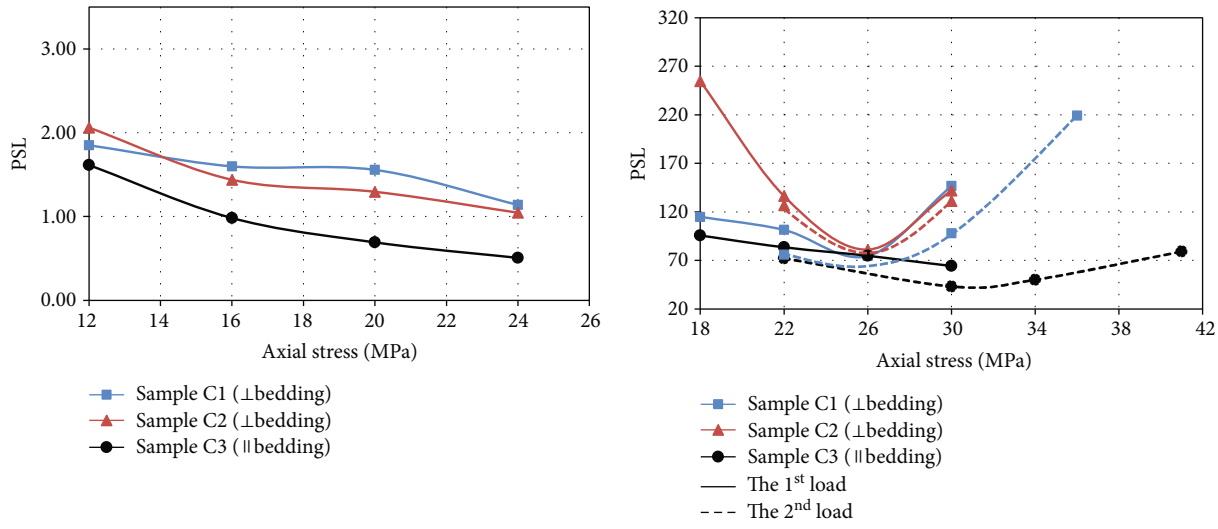

(a) Confining stress 8 MPa (b) Confining stress 14 MPa

Figure 10: The *PSL* calculating results under cyclic deviatoric stresses.

Table 4: The *EIP* and *SIP* calculated results under cyclic deviatoric stresses.

	Confining stress 8 MPa			The 1st load cycle of confining stress 14 MPa			The 2nd load cycle of confining stress 14 MPa		
	Sample C1	Sample C2	Sample C3	Sample C1	Sample C2	Sample C3	Sample C1	Sample C2	Sample C3
EIP (MPa^{-1})	0.028	0.028	0.015	0.022	0.031	0.012	0.023	0.014	0.011
SIP	9.635	8.629	4.840	25.465	18.227	5.774	25.303	19.518	4.376

Figure 8 illustrates the evolution of intrinsic permeability with cyclic axial strain. From Figure 8, it can be observed that intrinsic permeability decreases gradually as the strain rises, and when the strain recovers, intrinsic permeability is lower than it was during the loading process. Plastic deformation happens to coal's internal solid skeleton under external stresses, which leads to permanent damage.

The *PEL* and *PSL* calculated results of coal samples under cyclic deviatoric stresses are shown in Figures 9 and 10, respectively. During the process of increasing axial stress when confined stress is kept at 8 MPa and in the early stages of confined stress at 14 MPa, *PEL* and *PSL* decrease gradually. *PEL* and *PSL* of coal samples perpendicular to the bedding are commonly greater than those that are horizontal.

As axial stress increases, the sensitivity of intrinsic permeability decreases, and there is a loss of porosity or intrinsic permeability when unit strain decreases. In addition, the stress sensitivity of vertical intrinsic permeability is greater than horizontal. As depicted in Figures 9(b) and 10(b), the *PEL* and *PSL* curves have minimum values except the 1st loading process of sample C3. The extreme points of *PEL* and *PSL* in different directions are not the same, and the samples that are perpendicular to the bedding reach the minimum point near the axial stress of 26 MPa, while the minimum point in the horizontal direction is near 30 MPa. Beyond the minimum points, the intrinsic permeability becomes more and more sensitive to axial stress, and the porosity and permeability decrease sharply as the axial stress increases. The difference in axial stresses where extreme points in different directions are located is mainly attributed to the anisotropic mechanical characteristics of coal.

The permeability was tested under two stress cycles when confining stress was at 14 MPa. Figures 9(b) and 10(b) show that *PEL* and *PSL* of the 2nd loading process were all laid below the 1st for the same coal sample. This result indicates that the stress sensitivity of coal's intrinsic permeability and the loss of intrinsic permeability with unit strain during the 2nd loading process are smaller than the 1st one. It is speculated that the stress sensitivity of coal's intrinsic permeability will decrease as the applied loading cycles increase. This speculation needs to be further studied and confirmed.

The *EIP* and *SIP* calculated results under cyclic deviatoric stresses are listed in Table 4. The *EIP* and *SIP* of coal samples perpendicular to the bedding were all higher than the samples that were horizontal to the bedding when confining stress was at 14 MPa in the 1st loading cycle and when confining stress was at 8 MPa. After applying the same cyclic axial stress, the irreversible intrinsic permeability and the permanent damage of the vertical coal sample are obviously higher than the horizontal. The *EIP* and *SIP* results indicate that the ability of the internal structure in the vertical direction to resist the deformation induced by an external load is weaker than the ability of the horizontal direction.

In Table 4, the *EIP* and *SIP* of sample C2 of the 1st loading cycle are approximately two to three times higher than the 2nd loading cycle. For samples C1 and C3, because the peak stresses of the 2nd loading process are higher than the 1st, the differences in *EIP* and *SIP* between the two load cycles are small. Thus, the loss of intrinsic permeability during the 2nd load cycle is weaker than the 1st. It is speculated that the loss of intrinsic permeability decreases when the applied loading cycles increase, but that requires further study and confirmation.

5. Conclusions

The permeability of low-rank coal was tested by N_2 under cyclic loading conditions in different directions. Intrinsic permeability was obtained by calculating and removing the effect of gas slippage. By studying coal's intrinsic permeability and strain evolution during the cyclic loading process, this paper provides an understanding of the stress sensitivity of intrinsic permeability in different directions and the deformation characteristics of coal's internal structure. The main conclusions are listed below.

(1) To investigate the stress sensitivity of intrinsic permeability and the deformation characteristics during the loading process, the terms permeability stress-based loss rate (*PEL*) and permeability strain-based loss rate (*PSL*) are introduced. To describe the loss in intrinsic permeability and plastic or irreversible deformation features of the whole loading cycle, the terms stress-based irrecoverable permeability coefficient (*EIP*) and strain-based irrecoverable permeability coefficient (*SIP*) are introduced. This study uses these four parameters to quantitatively describe and interpret the changes in coal's internal structure

(2) *PEL* and *PSL* decrease sharply at the early stage of loading and then level off gradually. *PEL* and *PSL* of coal samples perpendicular to the bedding are commonly greater than those that are horizontal. The *PEL* and *PSL* curves have minimum values under deviatoric stresses. The extreme points of *PEL* and *PSL* in different directions are not the same. Beyond the minimum points, intrinsic permeability becomes more and more sensitive to axial stress, and the porosity and permeability decrease sharply as axial stress increases. The difference in extreme points of axial stress for different directions of the samples is mainly attributed to the anisotropic mechanical characteristics of coal

(3) Plastic deformation occurs to coal's internal solid skeleton under external stresses, leading to permanent damage. The *EIP* and *SIP* of coal samples perpendicular to the bedding are all higher than those that are horizontal. After being exposed to the same cyclic stresses, the vertical coal sample shows much higher irreversible intrinsic permeability and permanent damage than the horizontal. The ability of the internal structure in the vertical direction to resist deformation induced by an external load is weaker than that in the horizontal direction

Data Availability

The data used to support the findings of this study are included within the article.

Conflicts of Interest

The author declares that he has no conflicts of interest.

Acknowledgments

This study was supported and funded by the General Projects of Yunnan Basic Research Program (No. 202201AT070283).

References

[1] Z. J. Pan and L. D. Connell, "Modelling of anisotropic coal swelling and its impact on permeability behaviour for primary and enhanced coalbed methane recovery," *International Journal of Coal Geology*, vol. 85, no. 3-4, pp. 257–267, 2011.

[2] Z. C. Tang, Z. L. Wu, and J. P. Zou, "Appraisal of the number of asperity peaks, their radii and heights for three- dimensional rock fracture," *International Journal of Rock Mechanics and Mining Sciences*, vol. 153, article 105080, 2022.

[3] J. P. Zou, Y. Y. Jiao, F. Tan, J. H. Lv, and Q. Y. Zhang, "Complex hydraulic-fracture-network propagation in a naturally fractured reservoir," *Computers and Geotechnics*, vol. 135, article 104165, 2021.

[4] G. X. Wang, P. Massarotto, and V. Rudolph, "An improved permeability model of coal for coalbed methane recovery and CO_2 geosequestration," *International Journal of Coal Geology*, vol. 77, no. 1-2, pp. 127–136, 2009.

[5] J. Liu, Z. Chen, D. Elsworth, X. Miao, and X. Mao, "Linking gas-sorption induced changes in coal permeability to directional strains through a modulus reduction ratio," *International Journal of Coal Geology*, vol. 83, no. 1, pp. 21–30, 2010.

[6] F. G. Gu and R. Chalaturnyk, "Permeability and porosity models considering anisotropy and discontinuity of coalbeds and application in coupled simulation," *Journal of Petroleum Science and Engineering*, vol. 74, no. 3-4, pp. 113–131, 2010.

[7] Z. J. Pan, L. D. Connell, and M. Camilleri, "Laboratory characterisation of coal reservoir permeability for primary and enhanced coalbed methane recovery," *International Journal of Coal Geology*, vol. 82, no. 3-4, pp. 252–261, 2010.

[8] R. A. Koenig and P. B. Stubbs, "Interference testing of a coalbed methane reservoir," in *SPE Unconventional Gas Technology Symposium*, OnePetro, 1986.

[9] M. B. Wold and R. G. Jeffrey, "A comparison of coal seam directional permeability as measured in laboratory core tests and in well interference tests," in *SPE Rocky Mountain Regional Meeting*, OnePetro, 1999.

[10] T. Chaianansutcharit, H. Y. Chen, and L. W. Teufel, "Impacts of permeability anisotropy and pressure interference on coalbed methane (CBM) production," in *SPE Rocky Mountain Petroleum Technology Conference*, OnePetro, 2001.

[11] Z. J. Pan and L. D. Connell, "Modelling permeability for coal reservoirs: a review of analytical models and testing data," *International Journal of Coal Geology*, vol. 92, pp. 1–44, 2012.

[12] I. Palmer, "Coalbed methane completions: a world view," *International Journal of Coal Geology*, vol. 82, no. 3-4, pp. 184–195, 2010.

[13] F. D. Zhou, G. Q. Yao, Z. H. Tang, and D. O. Oyinkepreye, "Influence and sensitivity study of matrix shrinkage and swelling on enhanced coalbed methane production and CO2sequestration with mixed gas injection," *Energy Exploration and Exploitation*, vol. 29, no. 6, pp. 759–775, 2011.

[14] J. Q. Shi and S. Durucan, "Exponential growth in San Juan basin fruitland coalbed permeability with reservoir drawdown: model match and new insights," *SPE Reservoir Evaluation & Engineering*, vol. 13, no. 6, pp. 914–925, 2010.

[15] C. R. McKee, C. Bumb, and R. A. Koenig, "Stress-dependent permeability and porosity of coal and other geologic formations," *SPE Formation Evaluation*, vol. 3, no. 1, pp. 81–91, 1988.

[16] W. C. Zhu, J. Liu, J. C. Sheng, and D. Elsworthc, "Analysis of coupled gas flow and deformation process with desorption and Klinkenberg effects in coal seams," *International Journal of Rock Mechanics and Mining Sciences*, vol. 44, no. 7, pp. 971–980, 2007.

[17] J. Klinkenberg, "The permeability of porous media to liquids and gases," *Drilling and Production Practice*, vol. 2, pp. 200–211, 1941.

[18] Y. S. Wu, K. Pruess, and P. Persoff, "Gas flow in porous media with Klinkenberg effects," *Transport in Porous Media*, vol. 32, no. 1, pp. 117–137, 1998.

[19] S. E. Laubach, R. A. Marrett, J. E. Olson, and A. R. Scott, "Characteristics and origins of coal cleat: a review," *International Journal of Coal Geology*, vol. 35, no. 1-4, pp. 175–207, 1998.

[20] D. Jasinge, P. G. Ranjith, and S. K. Choi, "Effects of effective stress changes on permeability of Latrobe valley brown coal," *Fuel*, vol. 90, no. 3, pp. 1292–1300, 2011.

[21] J. P. Zou, W. Z. Chen, D. S. Yang, H. D. Yu, and J. Q. Yuan, "The impact of effective stress and gas slippage on coal permeability under cyclic loading," *Journal of Natural Gas Science and Engineering*, vol. 31, pp. 236–248, 2016.

[22] Y. Yang and F. D. Zhou, *Percolation Mechanism in Complex Reservoir with Low Permeability*, Xi'An Jiaotong University Press, 2010.

[23] S. Tao, Y. B. Wang, D. Z. Tang et al., "Dynamic variation effects of coal permeability during the coalbed methane development process in the Qinshui basin, China," *International Journal of Coal Geology*, vol. 93, no. 1, pp. 16–22, 2012.

[24] J. Zou, X. Hu, Y. Y. Jiao et al., "Dynamic mechanical behaviors of rock's joints quantified by repeated impact loading experiments with digital imagery," *Rock Mechanics and Rock Engineering*, vol. 55, no. 11, pp. 7035–7048, 2022.

[25] J. Zou, K. Wu, X. Zhang et al., "Effective evaluation of deep-hole blasting for controlling strong tremors induced by deep coal mining-a case study," *International Journal of Rock Mechanics and Mining Sciences*, vol. 159, article 105211, 2022.

[26] P. Tan, H. Pang, R. Zhang et al., "Experimental investigation into hydraulic fracture geometry and proppant migration characteristics for southeastern Sichuan deep shale reservoirs," *Journal of Petroleum Science and Engineering*, vol. 184, article 106517, 2020.